

# Temperature Correction on Shear Heating for the Viscosity of PP/Supercritical CO<sub>2</sub> Mixture at High Shear Rates

Hung-Yu Lan<sup>[1]</sup> and Hsieng-Cheng Tseng<sup>[2]</sup>

Department of Chemical Engineering, National Taiwan University of Science and Technology  
Taipei, Taiwan 106, R.O.C.

**Abstract**—The rheological behavior of PP/supercritical CO<sub>2</sub>(SCCO<sub>2</sub>) mixture at high shear rates was investigated with temperature correction in this study. An injection machine had been modified to generate the uniform CO<sub>2</sub>-containing PP melt. By measuring the pressure profile and flow rate of a slit die in front of the barrel during the injection procedure, and also monitoring the shear-induced temperature variation of the system, the dependence of viscosity on both shear rate and temperature then had been determined. A theoretical model based on the Cross model combined with the Eyring equation was proposed to correlate the shear-thinning behavior of PP/SCCO<sub>2</sub> mixture at various temperatures. The result revealed that the viscosity of PP melt was strongly influenced and reduced by the CO<sub>2</sub> addition. Under the same temperature, the viscosity was reduced more significantly at lower shear rates. However, as shear rates were raised, the viscosity reduction diminished and eventually reached a stable value at extremely high shear rates. Moreover, the viscosity reduction would be decreasing when the temperature was getting higher. For PP/CO<sub>2</sub> system, the correlation of viscosity data with shear rate at different temperatures could be well represented by a master curve.

*Key Words* : Rheology, Viscosity, Polymer, Supercritical fluid, Injection molding

## INTRODUCTION

In recent years, with special characters (McHugh, 1986), the supercritical fluid (SCF) has been widely utilized in the plastic foaming process as the replacement for conventional foaming agents. By manipulating the thermodynamic instability and controlling the spontaneous phase separation, an extremely high population density of up to  $10^9$ - $10^{15}$ /cm<sup>3</sup> of micro-bubbles with dimension of 1-100  $\mu$ m can be obtained in batch procedure either by temperature raise (Martini, 1981; Colton and Suh, 1987a, 1987b) or by pressure release (Goel, 1993; Parks, 1995; Arora, 1999). For improving the efficiency of process, the continuous operation was also under development (Park, 1993). As the rheological property of the Polymer/SCF mixture governs the operation conditions as well as the morphology and the quality of the final products, therefore, understanding the rheology of the mixture is of fundamental importance for both the theoretical development and the industrial application.

The basic flow behavior of the blowing agent/polymer mixtures had been examined in foam extrusion process by Han and Villamizar (1978), Yoo and

Han (1981) in the early stage. By installing a slit die with glass window at the front of an extruder, it was found that the gas-charged polymer melt exhibited a curved pressure profile along the axial direction near the die exit, but the polymer without the blowing agent showed a linear profile. He proposed that the gas separation and bubble growth within the die were responsible for the observed curvature variance. Gerhardt (1994) then adapted a Back Pressure Assembly on a capillary extrusion rheometer to prevent the formation of gas separation. The investigation on PDMS(Poly-dimethylsiloxane)/SCF system showed that the viscosity of PDMS decreased with the increase of CO<sub>2</sub> content, however, the shape of the flow curve looked similar to pure PDMS. Gendron and Daigneault (1997) also utilized a commercial on-line rheometer to measure PP(polypropylene)/CO<sub>2</sub> and PS(poly-styrene)/CO<sub>2</sub> systems. The results revealed that the addition of CO<sub>2</sub> could plasticize the polymers and depress the glass temperature ( $T_g$ ). The correlation of zero-shear viscosity with temperature variation was well expressed by the generalized Arrhenius/Williams-Landel-Ferry (W-L-F) equation.

In the following, many related researches utilizing equipments similar to Han's to carry out the

<sup>[1]</sup> 藍宏裕

<sup>[2]</sup> 曾憲政, To whom all correspondence should be addressed

studies. Lee *et al.* (1997) investigated a PS/CO<sub>2</sub> system and presented that the viscosity of polymer melt decreased with the increase of the gas amount, but it increased with the raise of pressure. Furthermore, Lee *et al.* (1998a, 1998b) performed the experiment on a PE(polyethylene)/PS blending system, and proposed utilization of the generalized Cross-Carreau model to correlate the viscosity dependence on the temperature, the pressure, the gas content, and the shear rate. Their results revealed that the shear-thinning behavior of polymer melt was less sensitive as CO<sub>2</sub> was added. Khan *et al.* (1998) showed that the viscosity of the Newtonian plateau was lower for polymer/gas mixture and spread out over a wider range, then the transition from Newtonian plateau to shear thinning occurred at a higher shear rate. Elkovich *et al.* (1998) also measured the viscosity variation of a PS/CO<sub>2</sub> system, and reported that a 56% viscosity reduction could be made by CO<sub>2</sub> addition for PS. After improving the mixing efficiency by using a twin-screw extruder, Lee *et al.* (1999a) extended the measured shear rate to a higher range. They proposed that the viscosity reduction for PS/CO<sub>2</sub> was more apparent than PE/CO<sub>2</sub> because the operation temperature was closer to the glass temperature of PS, so it enhanced the efficiency of dissolution of CO<sub>2</sub> in the PS system. In addition, some comparisons for various viscosity models had been made for PS/CO<sub>2</sub> system in the same year (Lee *et al.*, 1999b, 1999c). Kwag *et al.* (1999) again repeated the experiment of Gerhardt by using PS melt to replace PDMS. He reported that for three different systems, similar effect of dissolved gas component on rheological behavior were observed to follow roughly the same tendency with composition variation. Royer *et al.* (2000) measured the viscosity of PS/CO<sub>2</sub> system and presented that the viscosity of PS could be reduced 80% by CO<sub>2</sub> addition. By combining the traditional free volume theory with the thermodynamic model, the W-L-F equation was used to simplify the correlation for viscosity reduction of the mixture, and only the physical properties of pure material were needed in calculation. Again, Royer *et al.* (2001) extended their work to PP and LDPE (low density polyethylene), and proposed that the Arrhenius model could be used to correlate the temperature effect of melt viscosity for semi-crystalline materials.

To summarize, most of the past studies on the rheological behavior of polymer/SCF systems were made by using a modified extrusion machine. But due to the constraint that the flow rates were induced by screw rotation of the extruder, the generated shear rates were always limited below the order of 1E3 1/s. In present study, the fast movement of the screw on an injection machine was utilized to generate a much higher pressure and flow rate, so the experiment was

extended to a highly Non-Newtonian region, and the range of tested shear rates were achieved as high as order of 1E4 1/s. Hence, detailed examination for rheological behavior at high shear rates could then be made. Moreover, the effect of viscous heating that took place at high shear rates, which seriously influenced the melt viscosity was also considered and corrected in this study.

## THEORETICAL MODELING

For the fluid flow through a slit die, the stress at the wall is (Brydson, 1981):

$$\tau_w = \frac{H}{2} \frac{\Delta P}{\Delta L} \quad (1)$$

The apparent shear rate is

$$\dot{\gamma}_{app} = \frac{6Q}{wH^2} \quad (2)$$

From the definition the viscosity becomes

$$\eta_{app} = \frac{\tau_w}{\dot{\gamma}_{app}} \quad (3)$$

where  $H$  is the slit height,  $\Delta P$  the pressure drop,  $L$  the length of the die,  $Q$  the volumetric flow rate, and  $w$  the die width. As generally the tendency of viscous behavior remained the same after the Rabionwitsch correction, the apparent viscosity was discussed here instead of the true viscosity.

The Cross model interprets well the shear-thinning behavior or so called "pseudo-plasticity" for non-Newtonian fluid that can be formulated as below (Kennedy, 1993):

$$\eta = \frac{\eta_0}{1 + C(\eta_0 \dot{\gamma})^{1-n}} \quad (4)$$

where  $\eta_0$  is the zero-shear viscosity,  $C$  and  $n$  are material parameters related to both the curvature of the viscosity profile and the slope in the power law region.

For semi-crystalline PP material at the operation temperature, the Eyring equation (Chen, 1985) should be used:

$$\eta_0 = B \exp\left(\frac{D}{T}\right) \quad (5)$$

where  $B$ ,  $D$  are material constants and  $T$  the temperature. After combining the Cross model with the

Eyring equation, the dependence of the viscosity on both the shear rate and the temperature could be expressed in the form:

$$\eta = \frac{B \exp\left(\frac{D}{T}\right)}{1 + C \left[ B \exp\left(\frac{D}{T}\right) \dot{\gamma} \right]^{1-n}} \quad (6)$$

All the parameters could be determined by non-linear regression of least squares method when the raw viscosity data at different shear rates and temperatures were obtained.

### EXPERIMENTAL

#### Equipment

A traditional 3.5 ounce injection machine with maximum 1260 kg/cm<sup>2</sup> injection pressure and 100 ton clamping force had been modified by equipping an extra gas port on the barrel and also using a specially designed screw. The CO<sub>2</sub> came from the gas cylinder was pressurized by an ISCO 260D precision syringe pump, and then forced into the barrel. The screw was specially made with a diameter of 36 mm and the compression ratio of 3:1. The length

had been extended to 28 *L/D* ratio and set up with a Maddox element at front position to enhance the mixing efficiency. The gas was introduced at the transition zone of the screw. A shut off valve was installed at the front of nozzle and was driven by a hydraulic system in manual mode. The valve was closed to avoid the leakage before melt injection, and it was opened when the injection stage started. The slit die with dimensions of 0.15 m in length, 0.02 m in width, and 0.00075 m in height was adapted. The major reasons for using such a high *L/H* ratio die were first to achieve a fully developed flow, and second to avoid the entrance effect as measured points on the die wall were far away from the entrance. Moreover, multi-measuring points could be sampled at one time. Four Kistler 6159A pressure transmitters that 30 mm apart from each other were installed inside the slit die. The first one was located at 10 mm away from the die exit, particularly to inspect the unusual occurrence of exit-effect at that region. Three temperature transducers were placed between every two pressure transmitters to record the thermal history of the melt. The location and movement of the screw were measured by using the Daytronic Linear Velocity Displacement Transducer (LVDT). All the detected signals were converted into voltages and amplified by a Kistler 5041E Charge Amplifier, and then transferred to Data Acquisition software DAQ-2000 on a personal computer. The whole equipment system is drawn in Fig. 1.

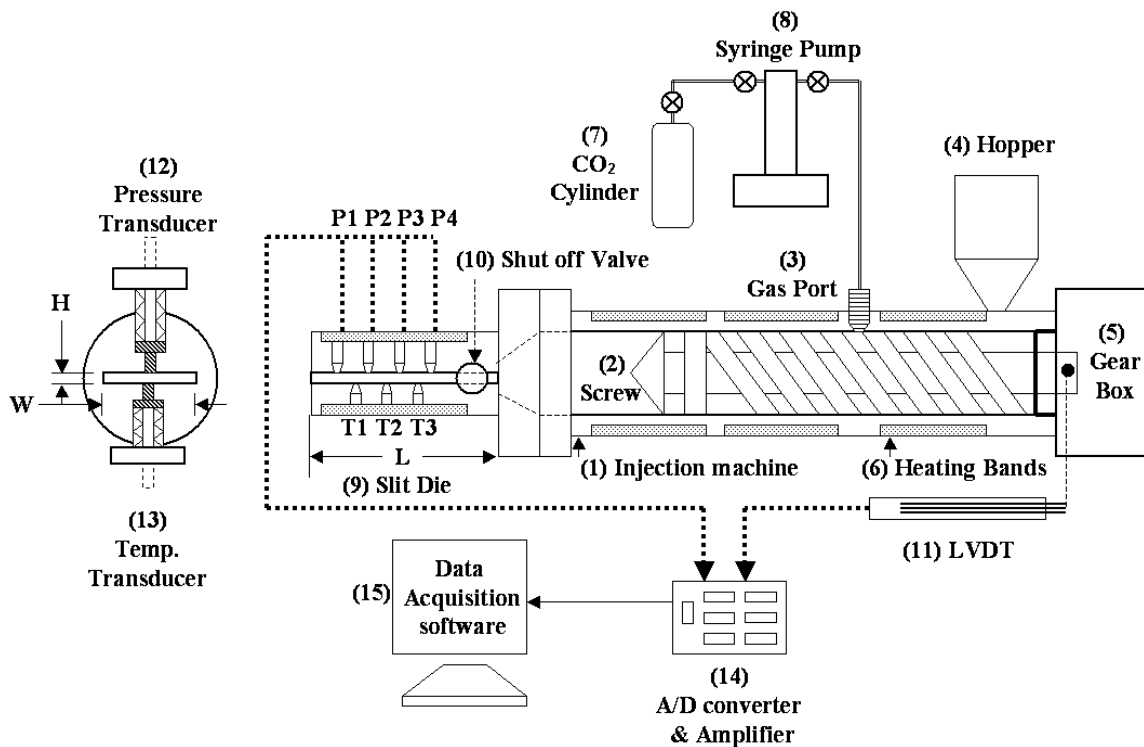


Fig. 1. Schematic diagram of the equipment that consists of the modified injection machine, the slit die, the gas supply and the data acquisition system.

## Materials

The PP polymer pellet, PP-7633 ( $M_w = 380,000$  and  $M_w/M_n = 4$ ) produced by Taiwan Polypropylene Co. was used in this study. The  $CO_2$  gas was supplied from San Yan Gas Co. with purity of 99%.

## Operation

As the compressibility of gas was very sensitive with pressure variation, the  $CO_2$  flow rate might vary significantly between different shuts if minor system fluctuation took place during the batch injection execution. Considering the injected gas amount was actually dominated by (1) the procedure operational time, (2) the pressure of gas input, and (3) the back pressure for polymer feed. So when the process was proceeding under the quasi-steady state in automatic mode, which meant that the three controlling parameters were all set fixed, then the gas charged amount could be regarded as the same at different shuts.

Three stages of temperature settings on the barrel were 185/200/210°C. When the gas was forced into the barrel, the mixture might not be uniform initially. But as the temperature and pressure escalated during transportation that generated by screw rotation, the gas converted into supercritical state and the mixing efficiency had been greatly improved. Finally, the uniform single-phase mixture would be formed. The gas pressure was set at 870 psi as the system kept stable and the injected samples were completely composed of uniform micro-bubbles. During the whole experiment, at least five procedures were repeated at each setting, and all the sampled data had been taken for correlation.

## RESULTS AND DISCUSSION

### Correction on the shear heating

As the injection machine offered a much higher pressure to achieve extreme high shear rates, unavoidably the performance of shearing itself generated heat within the melt, and thus it might change the temperature sufficient enough to reduce the viscosity and enhance the screw movement. So both the temperature and the shear rate variations during the injection stage had to be corrected. As an example, the relationship of screw location and injection time that were tested continuously at a specific pressure setting of 60% is depicted in Fig. 2. It shows that the location profile for each shut was not simply straight during the injection procedure. Actually the profile described the variation of screw location, and its slope illustrated the speed of the screw movement,

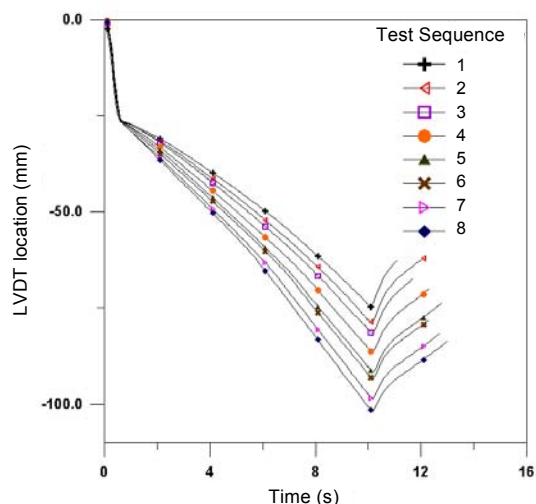


Fig. 2. The relationship of the LVDT location and the injection time for pure PP under continuous operations at the pressure setting of 60%.

and further the slope change implied the acceleration of screw motion. Under continuous operations, each shut had exactly the same starting point, but every shut was much faster than its previous one as the thermal energy was accumulated continuously. This situation could be explained by temperature effect as follows.

By measuring the temperature during the injection procedure, the data at T3 location was adapted as the melt temperature. And by the consequence with the LVDT location, the velocity of screw, the flow rate and the shear rate of melt could be calculated. The relationship of correlated shear rate with measured temperature is shown in Fig. 3. The plot reveals that the shear rate changes with the temperature rises during the shut, therefore, the correction on shear heating must be made in order to turn the measured viscosity into the same temperature base.

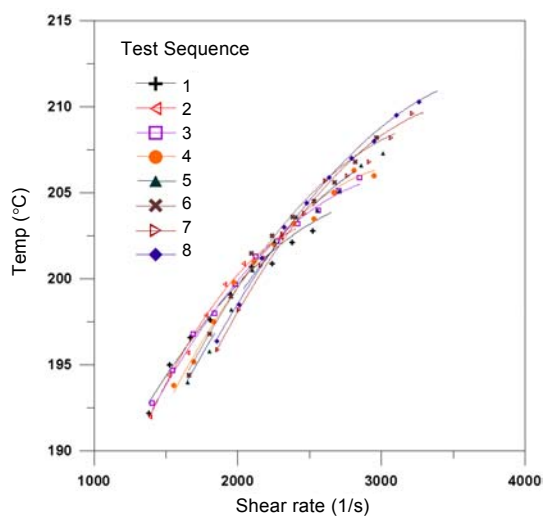


Fig. 3. The relationship of the temperature and the shear rate variation for pure PP at pressure setting of 60%.

**Pressure profile inside the slit die**

After measurement for pure PP material at different injection pressure settings, the pressure profiles inside the slit die are shown in Fig. 4. The straight dashed lines on the plot are obtained by linear regression and are representative for data at upstream, it means that the pressure gradients are reasonably constant at the flow channel that with a fixed cross section. But the data points near the die exit exhibit a distinct non-linear profile. This implies the exit-effect exists and the pressure decreases rapidly to normal atmosphere when the melt flows out of the die. Meanwhile, as the extrapolated pressure from straight-line region becomes negative at the die exit, the conventional method of Bagley correction for calculating the shear stress should be modified. In present study, the difference of pressure and the difference of axial distance at sampling points, P3 and P4, were adapted as the pressure drop and the effective flow length to calculate the shear stress that based on Eq. (1).

The same procedures were repeated for PP/CO<sub>2</sub> system, and the measured pressure data are presented in Fig. 5. Similarly, the pressure profiles are straight lines at upstream region and the area near die exit also exhibits non-linear relationship, but particularly there is a deflection between these two regions that can be clearly observed and be sketched qualitatively. The deflection was occurred as the pressure reduced to be insufficient to keep the gas soluble when gas-contained melt flows to a specified distance apart from die exit, then the gas phase separates and the bubble grows rapidly by diffusion. While the two-phase gas/melt solution forms, the flow resistance is raised and so the pressure gradient becomes higher. The locations of gas separation are also found to move toward closer to die exit as shear rates get higher.

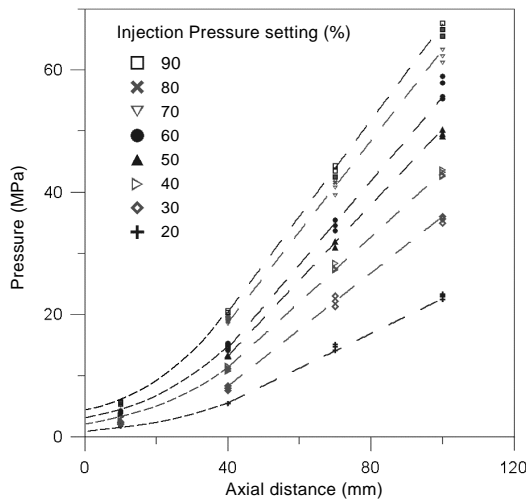


Fig. 4. Pressure profile along axial distance of the slit die for pure PP at different injection pressure settings.

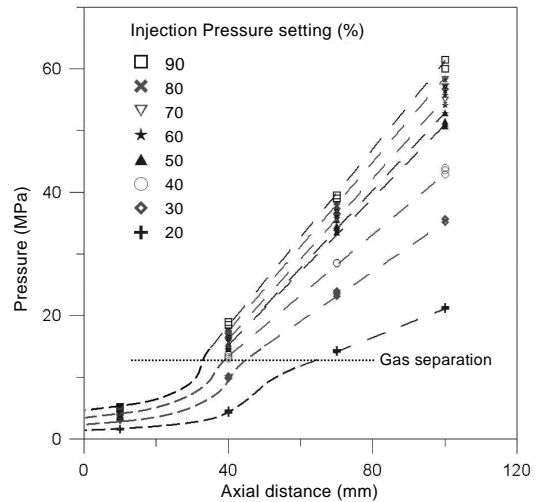


Fig. 5. Pressure profile along axial distance of the slit die for PP/CO<sub>2</sub> mixture at different injection pressure settings.

When the two-phase fluid flows further toward to the die exit, the exit-effect then dominants and the pressure gradient drops dramatically, hence the deflection occurs.

**Viscosity data and the best-fit result**

The raw measured data for viscosity related to temperature and shear rate of pure PP are displayed three dimensionally in Fig. 6. By this plot, the dependence of viscosity on both shear rate and temperature can be observed simultaneously. The surface on this plot represents the result of theoretical modeling within the tested range. All the parameters are estimated by nonlinear regression that using the Levenberg-Marquardt algorithm (Press *et al.*, 1990), and the best-fit values are shown in Table 1. From

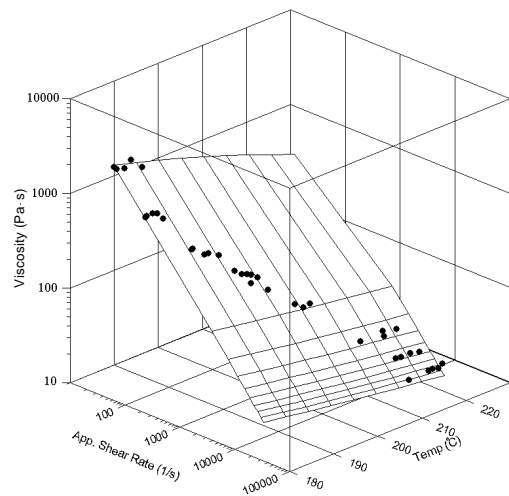


Fig. 6. Measured viscosity data and the regression surface for pure PP in three-dimensional coordination with respect to the shear rate and the temperature.

Table 1. Parameters based on the best fit of Eq. (6).

	$B$ (Pa·s)	$D$ (°C)	$C$	$n$	Standard Deviation
PP	0.001749	2921.68526	0.000139	0.214236	8.25%
PP/CO <sub>2</sub>	0.032626	2183.55092	0.000140	0.214796	7.48%

the table, apparently the major differences between the two systems are parameters,  $B$  and  $D$ , which means that the zero shear viscosity has been changed explicitly. The standard deviations of the experimented data for both PP and PP/CO<sub>2</sub> systems are 8.25% and 7.48% respectively, which indicate that the validation for model fitting is very good.

For clear depiction, the raw data is then displayed on projection of the viscosity-shear rate plane in Fig. 7. This plot apparently explicates the behavior of shear thinning for PP melt. The small error bars shown on the plot reveal that the deviations between the experimented data and predicted values are acceptable. It is found that even the operational temperature settings are all the same during the whole experiment, the measured points still show the trend that the melt temperature rises at higher shear rates, which is the evidence for the effect of shear heating. For inspecting the viscosity profiles that were based on the same temperature, the numerical calculation was conducted. The regression results, which are the lines shown on the plot, reveals that the melt viscosity decreases as shear rate increase, and also the viscosity variation with shear rate change is less sensitive at higher temperatures.

By rearranging the coordination, the data of pure PP are displayed on projection of viscosity-temperature plane in Fig. 8, then the variations of viscosity with temperature at constant shear rates are depicted. It shows that the melt viscosity is reduced

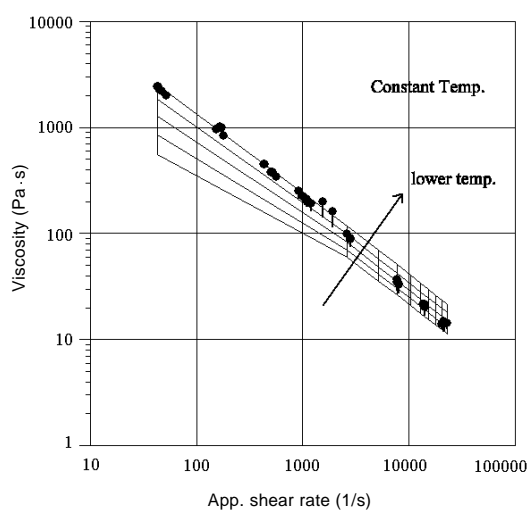


Fig. 7. The viscosity data for PP at different shear rates. Solid lines represent the regression calculation for constant temperatures.

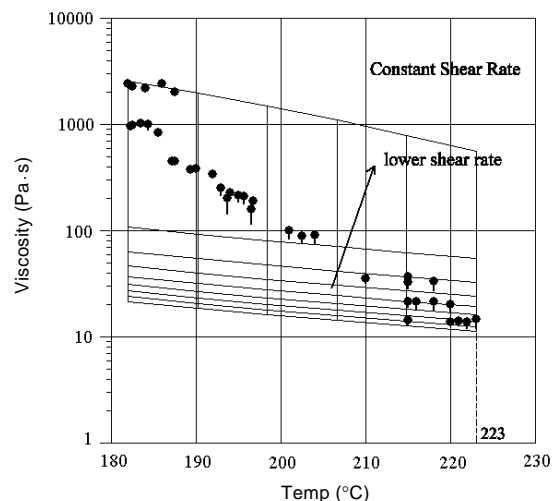


Fig. 8. The viscosity data for PP at different temperatures. Solid lines represent the regression calculation for constant shear rates.

as the temperature increases. Moreover, at low shear rates the tendency of viscosity variation with temperature change is more significant than at high shear rates.

The viscosity-shear rate relationship for the PP/CO<sub>2</sub> system then is depicted in Fig. 9 as the same procedures were repeated. Similar shear thinning behaviors are observed, and the temperature raise is also detected which indicates that the viscous heating is still existing and apparent for PP material with the CO<sub>2</sub> addition. Because the procedures were not conducted under the same temperature, the substantial consequence that SCF content acts on PP melt viscosity can not be clarified yet and will be explained as follows.

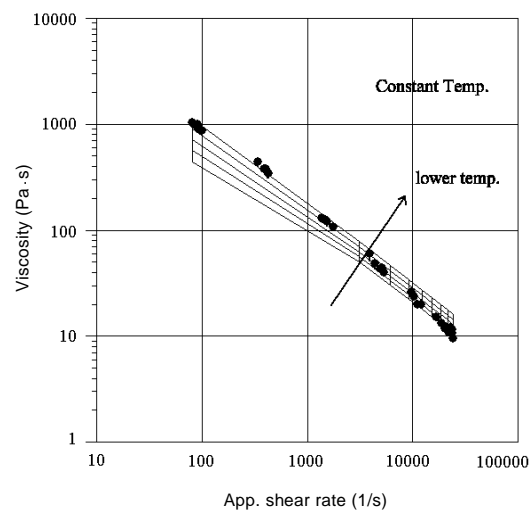


Fig. 9. The viscosity data for PP/CO<sub>2</sub> at different shear rates. Solid lines represent the regression calculation for constant temperatures.

The viscosity-temperature relationship for the PP/CO<sub>2</sub> system is shown in Fig. 10. It shows the similar trend that viscosity decreased as temperature increased. But based on the same setting for melt temperature, the highest temperature measurement is 216°C in this plot, which is lower than 223°C of pure PP in Fig. 8. This means that generally, the shear heating for this system was smaller than that in the pure PP system because the CO<sub>2</sub> content offers the lubrication effect to reduce the friction when melt flows.

By calculation using Eq. (6), the relationship of viscosity with shear rate at constant temperature for both systems is depicted and compared in Fig. 11. The lower limit shown on plot was obtained by extrapolation to a lower range of shear rates for presenting the zero-shear viscosities, and now the variation of the viscosity for both systems is concisely examined under the same conditions. The plot displays the Newtonian plateau at low shear rates, and all viscosity profiles show similar shear thinning behavior, but the transition point to the nonlinear region has extended to higher shear rates for PP/CO<sub>2</sub> system. As the temperature is higher, the critical shear rate also moves to a higher value. Actually, the slope of the profiles implies the sensitivity of the viscosity variation with the shear rate change. For each profile, the slope shows increasing tendency as shear rate rises under the same temperature, and it approaches a straight line at higher shear rate range. At region of extremely high shear rates for both systems, the viscosity profiles are almost parallel with a certain difference. This reveals that the SCF content contributes a fixed amount to reduce the viscosity when molecule chains have been almost completely disentangled.

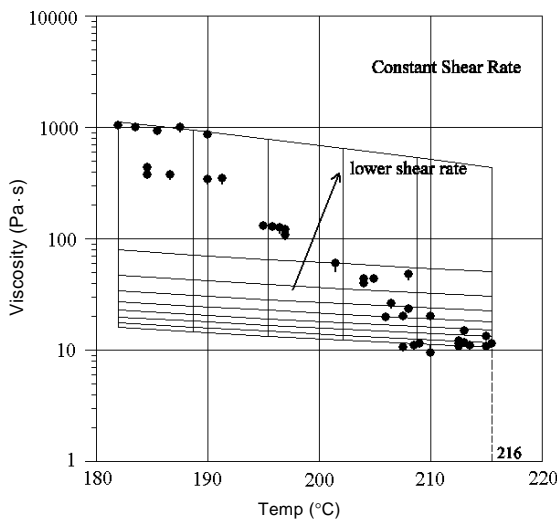


Fig. 10. The viscosity data for PP/CO<sub>2</sub> at different temperatures. Solid lines represent the regression calculation for constant shear rates.

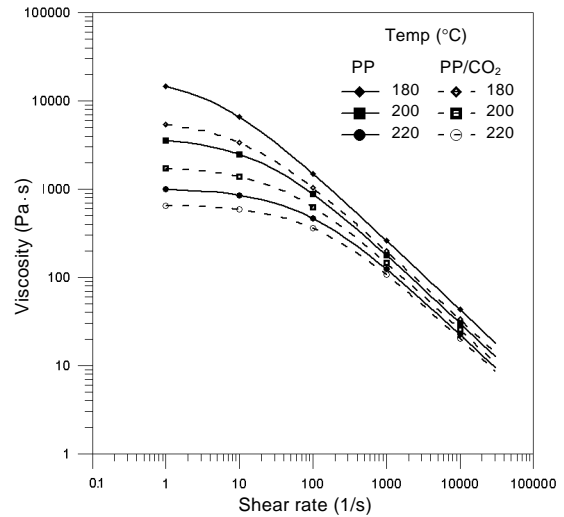


Fig. 11. The best-fit curves of viscosity with shear rate dependence at various temperatures for both systems.

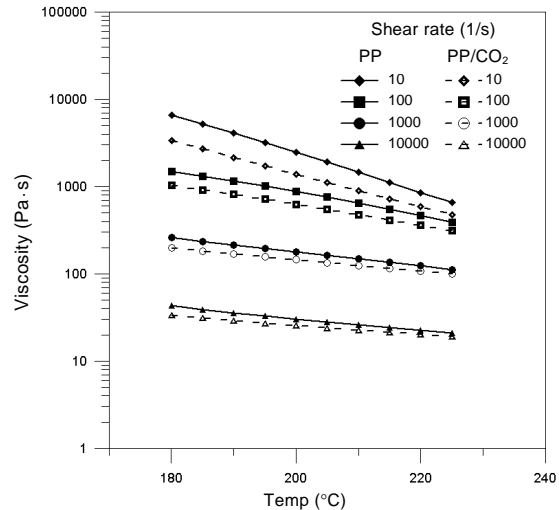


Fig. 12. The best-fit curves of viscosity with temperature dependence at various shear rates for both systems.

The viscosity-temperature relationship at constant shear rates for both systems then is depicted in Fig. 12. It shows the similar trend that viscosity decreases with temperature increase, and SCF provides the function for reducing PP viscosity at all temperatures and all shear rates. The slopes of profiles for PP/CO<sub>2</sub> system are always smaller than that for pure PP at the same condition, which means that the thermo-thinning behavior is less sensitive for PP after CO<sub>2</sub> added. At low shear rates, the viscosity dependence on temperature variation is always more significant than at high shear rates for both systems. At higher shear rates, the viscosity difference between the two systems then is getting smaller, which also implies that the contribution from SCF is diminished.

## Viscosity reduction

After the addition of CO<sub>2</sub>, the gas content becomes an extra factor that influences the viscosity of polymer, and it is now competitive to both original terms—the shear stress and the temperature. There are two mechanisms that SCF contributes to reduce the viscosity. Firstly, increase the system free volume to loosen the molecular attraction and secondly, reduce the density of molecular entanglement to decrease the flow resistance. But actually the extent of viscosity reduction is determined by whatever dominant mechanism is at different stages, because both factors exist at low shear rates but only free volume term remains at high shear rates.

The term of viscosity reduction had been defined as below for comparing the viscosity change after addition of SCF:

$$R = \frac{\eta_{pp} - \eta_{scf}}{\eta_{pp}}, \quad (7)$$

where  $\eta_{pp}$ ,  $\eta_{scf}$  denotes the viscosity of pure PP and PP/SCF respectively. The viscosity reduction itself represents the contribution from SCF content, and the relationship of viscosity reduction with shear rate at constant temperatures for both systems is shown in Fig. 13. It is found that the viscosity reductions are most evident at low shear rates for all temperatures. Similar observations that had been reported for PS and PE in literature (Lee *et al.*, 1999a) were presented on the same plot for comparison. The R-value, value of viscosity reduction, is higher as temperature is lower at specified shear rate. For example, the maximum viscosity reduction can achieve 63% at 180°C, but when temperature increases, the R-value decreases to 34% at 220°C. Alternatively, the viscosity reduction is also decreased as shear rates increase, but it behaves in different trends at different shear rates ranges. At low shear rates, the value of viscosity reduction is very high, but the decreasing tendency is also very sharp. As the shear rate increases, the trend of decreasing then is slower, and finally the R-value achieves a stable value at extremely high shear rates.

For explicit exploring the viscosity changes in the whole range of shear rate, the viscosity reduction is plotted on the semi-log coordination in Fig. 14. From the plot, it shows the tendency of viscosity reduction which is very dramatic at low sheared state, as in region I, because the SCF contributes greatly. But when the shear rate rises further, as in region II where the orientation of molecules has been enhanced by applying shear stress and also the molecular disentanglement has been started, the SCF contribution then becomes less important, so the viscosity reduction drops rapidly. When shear rates get even higher, as in region III, the shear stress term

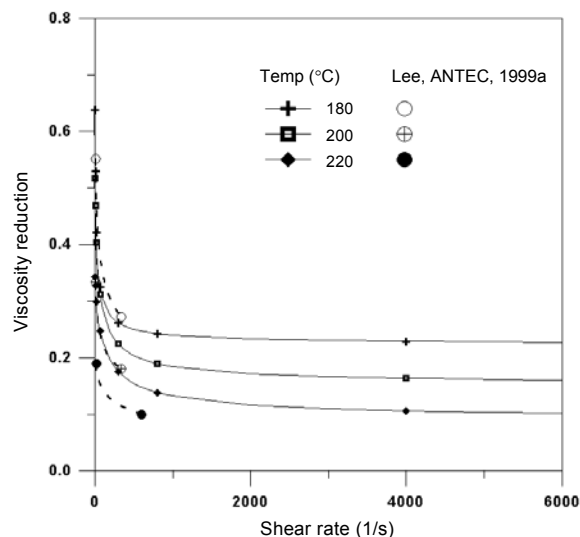


Fig. 13. The viscosity reduction for pure PP by CO<sub>2</sub> addition at different temperatures.

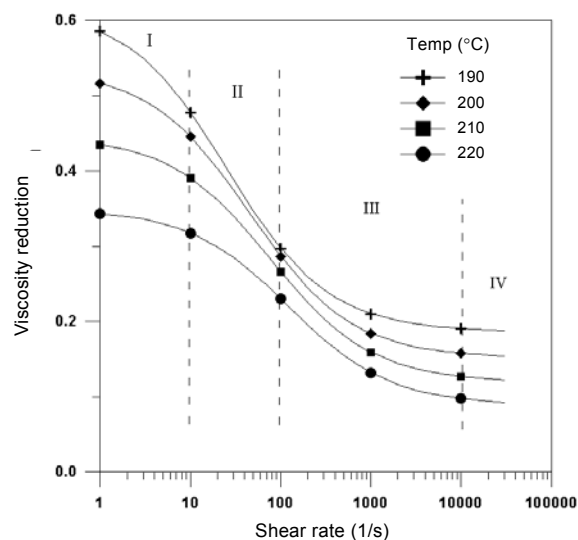


Fig. 14. The viscosity reduction of pure PP by CO<sub>2</sub> addition in semi-log coordination.

becomes the dominant factor, and the contribution from SCF is getting relatively minor, therefore the reduction value decreases further. At the region of extremely high shear rates, as in region IV, the value of viscosity reduction roughly approaches to a stable and final fixed value, which implies the limited influence remained that SCF contributes by adding extra free volume whenever the molecules have been almost completely oriented. Moreover, the viscosity reduction is decreasing as temperature increases at a specified shear rate, because SCF contributes relatively more when the molecules are frozen and then hardly moving at a lower temperature. But when the temperature rises, the molecular motions are much more active, so the contribution from SCF becomes less and then the related viscosity reduction decreases.

As viscosity profiles are similar in shape for both systems, the invariant master curve can be plotted in terms of reduced variables:  $(\eta/\eta_0)$  and  $\eta_0 \cdot \dot{\gamma}$  (Hieber and Chiang, 1992). After shifting the viscosity data from different temperatures, the master curve for PP and all experimented point are depicted in Fig. 15. As illustrated in this figure, the distribution of all data is closely collapsed to the master curve. This indicates that the viscosity change of PP melt with CO<sub>2</sub> addition can be regarded as mainly reflecting through the change of zero shear viscosity without influencing the other material constants, so the profile of the viscosity curve was not varied.

From alternative form of the Cross model,

$$\eta = \frac{\eta_0}{1 + \left(\frac{\eta_0}{\tau^*} \dot{\gamma}\right)^{1-n}}, \quad (8)$$

it can be shown that the parameters  $C$  and  $n$  are related to  $\tau^*$  which characterizes the shear stress level at that  $\eta$  is in the transition between Newtonian and power law regions (Hieber and Chiang, 1992).

$$\tau^* = 1/C^{1/(1-n)}. \quad (9)$$

According to Table 1, the derived values of  $\tau^*$  for PP and PP/CO<sub>2</sub> are  $8.10 \times 10^4$  Pa and  $8.09 \times 10^4$  Pa respectively, which are very close to the estimated value,  $8.0 \times 10^4$  Pa from Fig. 15.

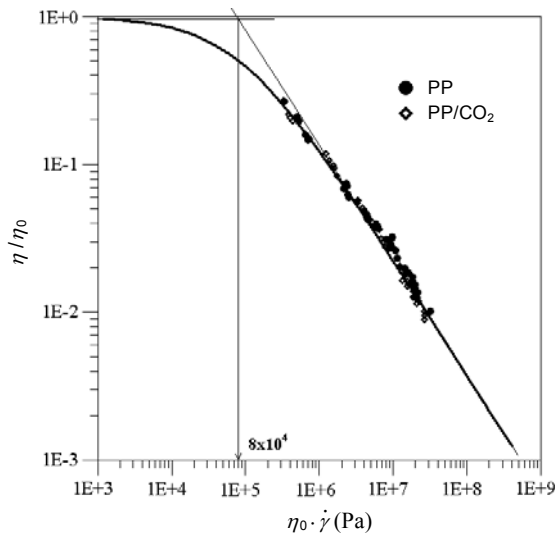


Fig. 15. The master curve that based on the Cross model for PP and scattering of all the data points.

### CONCLUSION

A traditional injection machine has been modified to make investigation on rheological behaviors

for PP/SCCO<sub>2</sub> mixture at a highly Non-Newtonian range. The order of shear rates achieved was as order 1E4 1/s. The shear-induced temperature variations at high shear rates were considered and corrected. It was observed that the pressure profile for pure PP melt within the slit die could be represented by a straight line at the region far above the die exit, and it showed a non-linear profile at the die exit as the consequence of exit-effect. A special deflection was found for PP/CO<sub>2</sub> mixture at the region near the die exit, which exhibited the influence of gas separation. Theoretically, the Cross model for expression of shear thinning behavior and the Eyring equation for describing the temperature dependence of zero shear viscosity were combined to correlate the viscosity for both systems. The results showed that, by SCF addition, the viscosity of PP was effectively reduced as increase of the system free volume and decrease of the density of molecular entanglement. The viscosity reduction was most apparent at low temperatures and low shear rates. As shear rate or temperature increased, the SCF contribution decreased, finally the viscosity reduction achieved a stable value at extremely high shear rates. After scaling out the temperature and the SCF effects, the master curve could well represent the distribution of all the experimented data.

### ACKNOWLEDGEMENT

Financial support from the National Science Council of Taiwan, the Republic of China is gratefully acknowledged (NSC 89-2216-E-011-050).

### NOMENCLATURE

$B$	parameter of Eyring equation, Pa · s
$C$	parameter of Cross model
$D$	parameter of Eyring equation, °C
$H$	height of slit die, m
$L$	length of slit die, m
$n$	parameter of Cross model
$P$	pressure, Pa
$Q$	volumetric flowrate, m <sup>3</sup> /s
$R$	viscosity reduction
$T$	temperature, °C
$w$	width of slit die, m

### Greek symbols

$\Delta P/\Delta L$	pressure gradient, Pa/m
$\eta$	viscosity, Pa · s

$\eta_0$	zero shear viscosity, Pa·s
$\eta_{app}$	apparent viscosity, Pa·s
$\eta_{pp}$	viscosity of PP, Pa·s
$\eta_{scf}$	viscosity of PP/SCF mixture, Pa·s
$\dot{\gamma}_{app}$	apparent shear rate, 1/s
$\tau^*$	transition stress, Pa
$\tau_w$	shear stress at wall, Pa

## REFERENCES

- Arora, K. A., "Preparation and Characterization of Microcellular Foams Processed in Supercritical Carbon Dioxide," Ph.D. Dissertation, Department of Polymer Sci. Eng., U. of Massachusetts Amherst, U.S.A. (1999).
- Brydson, J. A., *Flow Properties of Polymer Melts*, ISBN: 0-7114-5681-X (1981).
- Chen, T. Y., "Analysis of Heat Transfer of Polymer Melt in Capillary Tube and Its Application to the Analysis of Rheological Data," S.M. Thesis, Department of Chem. Eng., National Taiwan Institute of Technology, Taiwan, R.O.C. (1985).
- Colton, J. S. and N. P. Suh, "The Nucleation of Microcellular Thermoplastic Foam with Additives: Part I: Theoretical Considerations," *Polym. Eng. Sci.*, **27**, 485 (1987a).
- Colton, J. S. and N. P. Suh, "The Nucleation of Microcellular Thermoplastic Foam with Additives, Part II, Experimental Results and Discussion," *Polym. Eng. Sci.*, **27**, 493 (1987b).
- Elkovitch, M. D., L. J. Lee, and D. L. Tomasko, "Viscosity Reduction of Polymers by the Addition of Supercritical Carbon Dioxide in Polymer Processing," *SPE ANTEC*, p.1407 (1998).
- Gendron, R. and L. E. Daigneault, "Rheological Behavior of Mixtures of Various Polymer Melts with CO<sub>2</sub>," *SPE ANTEC*, p.1096 (1997).
- Gerhardt, L. J., "A Rheological Investigation of Polydimethylsiloxane Swollen with Supercritical Carbon Dioxide," Ph.D. Dissertation, Department of Chem. Eng., U. of Wayne State, U.S.A. (1994).
- Goel, S. K., "A Pressure-Based Method of Generating Microcellular Polymers Using Supercritical Carbon Dioxide as Foaming Agent," Ph.D. Dissertation, U. of Pittsburgh, U.S.A. (1993).
- Han, C. D. and C. A. Villamizar, "Studies on Structure Foam Processing, I. The Rheology of Foam Extrusion," *Polym. Eng. Sci.*, **18**, 687 (1978).
- Hieber, C. A. and H. H. Chiang, "Shear-Rate-Dependence Modeling of Polymer Melt Viscosity," *Polym. Eng. Sci.*, **32**, 931 (1992).
- Kennedy, P., *Flow Analysis Reference Manual*, Moldflow Pty. Ltd. (1993).
- Khan, V., C. Kwag, C. W. Manke, and E. Gulari, "Supercritical Fluids as Polymer Processing Aids," *SPE ANTEC*, p.1418 (1998).
- Kwag, C., C. W. Manke, and E. Gulari, "Rheology of Molten Polystyrene with Dissolved Supercritical and Near-Critical Gases," *J. Polym. Sci., Part B: Polym. Phys.*, **37**, 2771 (1999).
- Lee, M., C. B. Park, and C. Tzoganakis, "On-Line Measurement of PS/CO<sub>2</sub> Solution Viscosities," *SPE ANTEC*, p.1991 (1997).
- Lee, M., C. B. Park, and C. Tzoganakis, "Modeling of PS/Supercritical CO<sub>2</sub> Solution Viscosities," *SPE ANTEC*, p.1902 (1998a).
- Lee, M., C. Tzoganakis, and C. B. Park, "Extrusion of PE/PS Blends with Supercritical Carbon Dioxide," *Polym. Eng. Sci.*, **38**, 1112 (1998b).
- Lee, M., C. Tzoganakis, and C. B. Park, "Extrusion of PE/PS Blends with Supercritical CO<sub>2</sub> in a Twin-Screw Extruder and a Twin/Single Tandem System," *SPE ANTEC*, p.2806 (1999a).
- Lee, M., C. B. Park, and C. Tzoganakis, "Measurements and Modeling of PS/Supercritical CO<sub>2</sub> Solution Viscosities," *Polym. Eng. Sci.*, **39**, 99 (1999b).
- Lee, M., C. B. Park, C. Tzoganakis, and H. E. Naguib, "Comparison of Various Viscosity Models for PS/CO<sub>2</sub> Solutions," *SPE ANTEC*, p.1241 (1999c).
- Martini, J. E., "The Production and Analysis of Microcellular Foam," S.M. Thesis, Department of Mechanical Eng., U. of Mass. Inst. Tech., U.S.A. (1981).
- McHugh, M. A., *Supercritical Fluid Extraction: Principles and Practice*, Butterworths, Boston, U.S.A. (1986).
- Park, C. B., "The Role of Polymer/Gas Solutions in Continuous Processing of Microcellular Polymers," Ph.D. Dissertation, Department of Mechanical Eng., U. of Mass. Inst. Tech., U.S.A. (1993).
- Parks, K. L., "Generation of Microcellular PU via Polymerization in CO<sub>2</sub>," Ph.D. Dissertation, U. of Pittsburgh, U.S.A. (1995).
- Press, W. H., B. P. Flannery, D. A. Teukolsky, and W. T. Vetterling, *Numerical Recipes in C*, Cambridge University Press (1990).
- Royer, J. R., Y. J. Gay, J. M. Desimone, and S. A. Khan, "High-Pressure Rheology of Polystyrene Melts Plasticized with CO<sub>2</sub>: Experimental Measurement and Predictive Scaling Relationships," *J. Polym. Sci., Part B: Polym. Phys.*, **38**, 3168 (2000).
- Royer, J. R., J. M. Desimone, and S. A. Khan, "High Pressure Rheology and Viscoelastic Scaling Predictions of Polymer Melts Containing Liquid and Supercritical Carbon Dioxide," *J. Polym. Sci., Part B: Polym. Phys.*, **39**, 3055 (2001).
- Yoo, H. J. and C. D. Han, "Studies on Structural Foam Processing, III. Bubble Dynamics in Foam Extrusion through a Converging Die," *Polym. Eng. Sci.*, **21**, 69 (1981).

(Manuscript received Jan. 20, 2003, and accepted Apr. 28, 2003)

# 高剪率下聚丙烯／超臨界二氧化碳混合熔體黏度量測之 溫度修正探討

藍宏裕 曾憲政

國立台灣科技大學化學工程學系

## 摘 要

本文探討高剪率下 PP／超臨界二氧化碳混合熔體之流變行為，並考慮剪切熱引起之溫度修正。實驗使用改裝之射出成型機，以產生包含均勻 CO<sub>2</sub> 氣體之 PP 熔體；再藉由量測射出動作時料管前端狹縫模頭內之壓力分佈與體積流率，並隨時監測溫度變化，則黏度數據與剪率及溫度之關聯性可以獲得檢驗。理論部分是以 Cross model 結合 Eyring equation，得以對此混合物質在各不同溫度下之剪稀薄特性進行良好描述。結果顯示，PP 熔體之黏度深受添加之 CO<sub>2</sub> 成份影響，在相同溫度時，低剪率下之黏度降低較顯著，但隨剪率升高，黏度降會逐漸減小，而最終在極高剪率下趨於一穩定值；而黏度下降情形也是隨溫度升高而減小；對此 PP/CO<sub>2</sub> 系統在不同溫度、剪率下之黏度值，藉由主曲線之描述仍可獲致相當良好代表性。